Cell

Regulation of Vertebrate Nervous System Alternative Splicing and Development by an SR-Related Protein

John A. Calarco,[1,2] Simone Superina,[2,3] Dave O'Hanlon,[1] Mathieu Gabut,[1] Bushra Raj,[1,2] Qun Pan,[1] Ursula Skalska,[1] Laura Clarke,[2] Danielle Gelinas,[3] Derek van der Kooy,[1,2] Mei Zhen,[2,4] Brian Ciruna,[2,3] and Benjamin J. Blencowe[1,2,5,*]
[1]Banting and Best Department of Medical Research, Donnelly Centre for Cellular and Biomolecular Research, University of Toronto, 160 College Street, Toronto, Ontario M5S 3E1, Canada
[2]Department of Molecular Genetics, University of Toronto, 1 King's College Circle, Toronto, Ontario M5S 1A8, Canada
[3]Program in Developmental and Stem Cell Biology, The Hospital for Sick Children, 555 University Avenue, Toronto, Ontario M5G 1X8, Canada
[4]Samuel Lunenfeld Research Institute, Mount Sinai Hospital, 600 University Avenue, Toronto, Ontario M5G 1X5, Canada
[5]Centre for Bioinformatics, King's College, University of London, Strand, London WC2R 2LS, UK
*Correspondence: b.blencowe@utoronto.ca
DOI 10.1016/j.cell.2009.06.012

SUMMARY

Alternative splicing is a key process underlying the evolution of increased proteomic and functional complexity and is especially prevalent in the mammalian nervous system. However, the factors and mechanisms governing nervous system-specific alternative splicing are not well understood. Through a genome-wide computational and expression profiling strategy, we have identified a tissue- and vertebrate-restricted Ser/Arg (SR) repeat splicing factor, the neural-specific SR-related protein of 100 kDa (nSR100). We show that nSR100 regulates an extensive network of brain-specific alternative exons enriched in genes that function in neural cell differentiation. nSR100 acts by increasing the levels of the neural/brain-enriched polypyrimidine tract binding protein and by interacting with its target transcripts. Disruption of nSR100 prevents neural cell differentiation in cell culture and in the developing zebrafish. Our results thus reveal a critical neural-specific alternative splicing regulator, the evolution of which has contributed to increased complexity in the vertebrate nervous system.

INTRODUCTION

Recent high-throughput sequencing studies indicate that at least 95% of human multiexon genes produce alternatively spliced transcripts (Pan et al., 2008; Wang et al., 2008). Alternative splicing (AS) has played a major role in the evolutionary expansion of proteomic and functional complexity underlying many cellular processes and is especially prevalent in the vertebrate nervous system, with emerging key roles in synaptogenesis, neurite outgrowth, axon guidance, ion channel activity, and long-term potentiation (Li et al., 2007; Ule and Darnell, 2006). However, mechanisms that control neural-specific AS and that underlie the evolution of increased nervous system complexity are poorly understood.

Regulated AS requires the interplay of *cis*- and *trans*-acting factors that repress or activate splice site selection (Blencowe, 2006; Wang and Burge, 2008). RNA binding domain (RBD)-containing proteins belonging to the heterogeneous nuclear ribonucleoprotein (hnRNP) family and a superfamily of alternating Arg/Ser (RS) domain-containing proteins, referred to as "SR family" and "SR-related" proteins, act widely to control AS. Members of these protein families can either repress or promote the formation of active splicing complexes (spliceosomes), often depending on the location of cognate binding sites within exon or intron sequences (Lin and Fu, 2007; Martinez-Contreras et al., 2007).

SR family proteins contain one or two N-terminal RNA recognition motifs and a C-terminal RS domain, whereas SR-related proteins, which include factors that are pivotal in the control of sex determination in *Drosophila*, contain RS domains but may or may not contain RBDs (Lin and Fu, 2007). Phosphorylated RS domains are thought to function in the formation of protein-protein and protein-RNA interactions required for spliceosome assembly (Shen et al., 2004; Wu and Maniatis, 1993). Approximately 40 mammalian RS domain proteins have been implicated in splicing (Lin and Fu, 2007). Although ubiquitously expressed, it has been proposed that variable levels of these proteins may contribute to cell- and tissue-dependent AS patterns (Hanamura et al., 1998; Zahler et al., 1993).

To date, only RBD proteins that lack RS domains have been shown to possess tissue-restricted expression patterns and several such proteins play important roles in cell- and tissue-specific AS (Li et al., 2007). These include the neuronal-specific Nova-1/2 and HuB proteins, the neuronal and muscle-expressed Fox-1/2, CELF/CUGBP, and MBNL family proteins, and the neural, myoblast, and testis-expressed nPTB protein (also referred to as brPTB and PTBP2). nPTB is a paralog of the widely expressed PTB (also hnRNPI/PTBP1) splicing repressor protein (Ashiya and Grabowski, 1997; Markovtsov et al., 2000; Polydorides et al., 2000). A switch from PTB to nPTB expression during

neuronal differentiation has been implicated in regulating neuronal AS (Boutz et al., 2007; Makeyev et al., 2007; Spellman et al., 2007). Previous evidence has suggested that this switch results in the formation of ''less repressive'' nPTB-bound splicing complexes that are responsive to positive-acting factors in neurons (Markovtsov et al., 2000). However, the mechanisms controlling neuronal-specific exon inclusion patterns in conjunction with nPTB have remained unclear.

Several tissue-restricted AS factors are involved in controlling subsets of exons that are enriched in functionally-related genes (Boutz et al., 2007; Kalsotra et al., 2008; Ule et al., 2005; Yeo et al., 2009; Zhang et al., 2008). For example, through binding to clusters of YCAY motifs distributed within specific exon and intron zones, Nova2 can positively or negatively regulate ~7% of neural-specific alternative exons in genes that function in the synapse and in axon guidance (Licatalosi et al., 2008; Ule et al., 2005). How AS specificity is established for the vast majority of other neural-specific exons is not understood, however. Moreover, the specific biological processes controlled by the majority of neural-specific exons are also not well understood.

We have identified a tissue- and vertebrate-restricted RS domain protein, referred to as the neural-specific SR-related protein of 100 kDa (nSR100). Knockdown of nSR100 disrupts the inclusion of a large set of nervous system-specific alternative exons that are significantly enriched in genes with critical functions in neural cell differentiation. Consistent with this molecular programming function, nSR100 is required for neural cell differentiation in vivo. nSR100 forges neural specificity in AS by activating nPTB expression and, in conjunction with nPTB, by binding directly to its regulated target transcripts. nSR100 thus acts in a multifaceted manner in the tissue-specific regulation of a network of exons associated with neural cell differentiation and the evolution of vertebrate nervous system complexity.

RESULTS

A Genome-wide Screen Identifies a Vertebrate and Neural-Specific SR-Related Protein

To identify mammalian SR-related proteins with the potential to function as cell type- and/or tissue-specific splicing regulators, we used a computational procedure for the genome-wide surveying of RS domain protein-encoding genes (Figure 1A; refer to the Supplemental Experimental Procedures available online). Applying this procedure to a set of nonredundant mouse cDNAs resulted in the identification of 112 known or putative new RS domain genes (see Table S1).

Manual annotation revealed that 36% (40/112) of the RS domain genes have a function associated with splicing and 15% (17/112) have functions associated with RNA polymerase II-dependent transcription and mRNA 3′-end processing, which are coupled to and can influence splicing (Figure 1A). Remarkably, 32% (36/112) of the identified genes have no annotated function. Given that more than one third of the annotated genes have known functions in splicing, many of the previously uncharacterized genes likely also participate in splicing. Moreover, since 96% (108/112) of the predicted mouse proteins encoded by these genes have a closely related human ortholog with a computationally defined RS domain, the majority of these proteins likely have conserved functions.

Using microarray profiling data we analyzed expression patterns of the computationally-mined RS domain genes in 50 diverse mouse cell and tissue types (Figures 1B and S1). Many of these genes appear to be widely but variably expressed, which is consistent with previous observations (Hanamura et al., 1998; Zahler et al., 1993). Interestingly, hierarchical clustering analysis reveals that two prominent subsets of genes display distinct spatiotemporal regulation. One subset displays elevated expression in whole embryo and embryonic head samples from days 9.5 to 14.5 and the other displays elevated expression in adult nervous system tissues (Figure 1B, boxed region; and Figure S1).

We focused our attention on an RS domain gene (*NM_026886*; human *NM_194286/KIAA1853*) displaying increased expression in the developing embryo and highly restricted expression in adult nervous system and sensory organ tissues (Figure 1B). The *NM_026886* open reading frame (ORF) is predicted to encode a 608 amino acid protein of 68 kDa that contains prominent runs of alternating SR/RS repeats (Figure 1C). Although the protein encoded by the *NM_026886* gene has not been functionally characterized, it has been detected as a tumor antigen in pediatric patients with medulloblastomas (Behrends et al., 2003).

In addition to its neural-restricted expression pattern, a feature of the *NM_026886 ORF* that distinguishes it from previously characterized RS domain proteins is that it is highly conserved only in vertebrate species (Figure S2 and data not shown). The *NM_026886* ORF and its orthologs lack a canonical RBD. The only region of significant similarity with other protein sequences is a sequence spanning amino acids 490 to 521 that is identical to amino acids 573 to 604 in the human SRm300 splicing coactivator subunit-like gene (SRm300-like/*SRRM2L*). These results, together with additional experiments described below, indicate that the *NM_026886* gene encodes the neural-specific SR-related protein of 100 kDa, which we refer to below as nSR100.

Distribution of nSR100

RT-PCR assays confirmed that nSR100 mRNA is strikingly enriched in multiple brain regions and sensory organ tissues (Figure 1D). A rabbit polyclonal antibody raised against a GST fusion protein containing amino acids 1 to 82 of human nSR100 recognizes a band that migrates at ~100 kDa in neuronal-derived cell lines (mouse Neuro2a and human Weri-RB1), but which is not expressed in nonneural mouse or human cell lines (C2C12, NIH 3T3, HEK293-T, and HeLa) (Figure 1E). The higher than expected mobility of nSR100 is typical of SR proteins because RS domains are generally highly phosphorylated. Confirming the phosphorylation status of nSR100, myc epitope-tagged nSR100 protein expressed in Neuro2a cells was detected using the monoclonal antibody mAb104, which specifically recognizes a phosphoepitope shared among SR proteins (data not shown; Zahler et al., 1992).

To establish whether nSR100 is expressed in specific neural cell types, adult mouse neural progenitor cells were differentiated in vitro into neurons and glia, the latter comprising astrocyte and oligodendrocyte populations. These neural cell populations were coimmunostained with anti-nSR100 antibody and anti-βIII

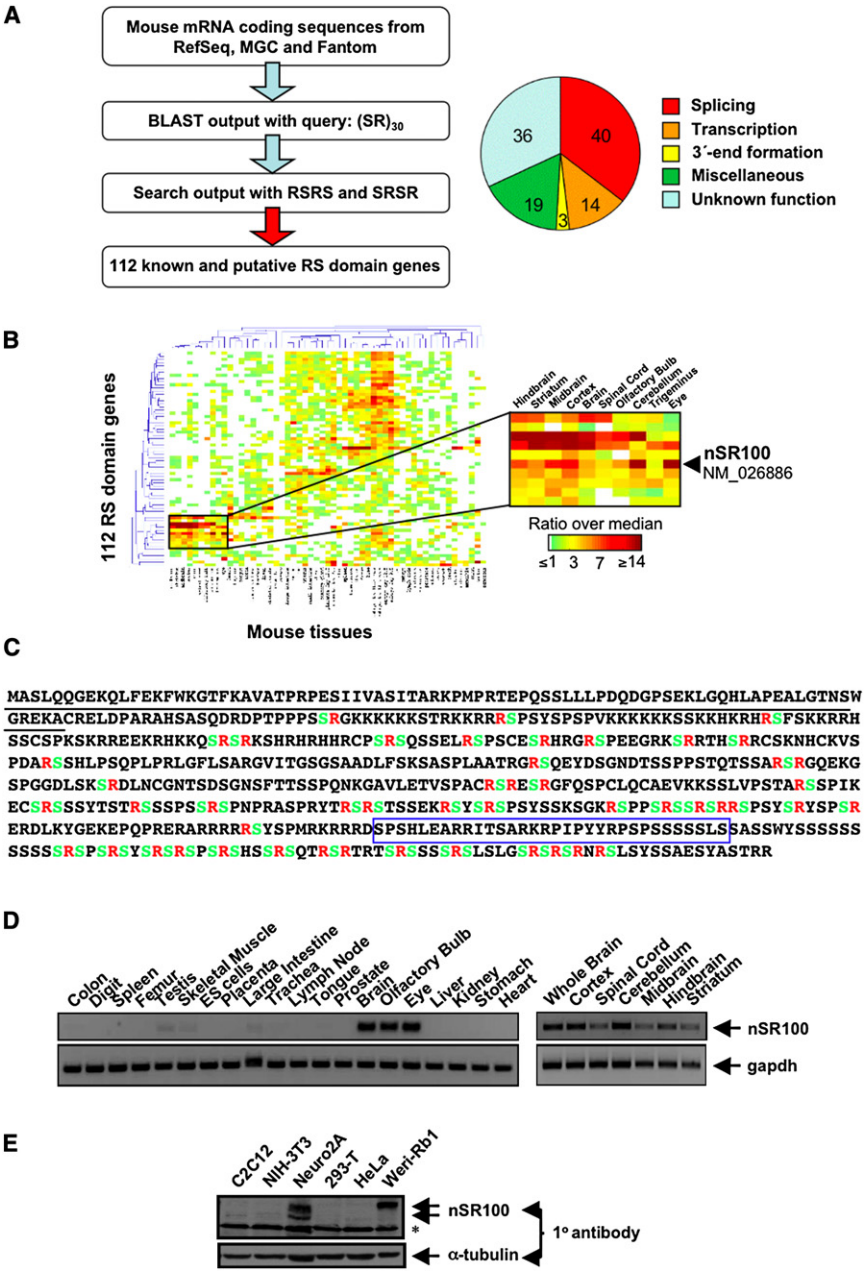

Figure 1. Identification and Expression Characteristics of nSR100

(A) (Left) Computational strategy for the genome-wide survey of mouse RS domain protein genes. (Right) Functional associations of computationally defined mouse RS domain protein genes (refer to Table S1 for a full list and description).

(B) Clustergram showing relative mRNA expression levels of RS domain protein genes (y axis) across 50 mouse cell and tissue types (x axis). Color scale indicates fold expression relative to the median value across the data set. The enlarged portion of the clustergram shows RS domain protein genes with elevated expression in neural tissues with NM_026886/Riken cDNA 1500001A10 (nSR100) indicated. Refer to Figure S1 for an enlarged view of the entire clustergram with all gene names indicated.

(C) Translated sequence of mouse nSR100 (from *NM_026886*), with RS/SR dipeptides highlighted. The underlined region indicates amino acids (1–82) used to generate an anti-nSR100 polyclonal antibody. The boxed region is identical to a sequence in the SRm300 splicing coactivator subunit-like protein (SRRM2L).

(D) RT-PCR analysis of mouse nSR100 mRNA expression across 20 diverse tissues and several brain subregions, relative to Gapdh mRNA expression in the same samples.

(E) Western blot of nonneuronal and neuronal-derived cell line lysates probed with an anti-nSR100 antibody. Arrowheads indicate detection of nSR100 (see also Figures 2 and 5) and the asterisk indicates a cross-reacting species.

tubulin (neuronal marker) or anti-glial fibrillary acidic protein (glial marker) antibodies. nSR100 is highly enriched in the nuclei of the neuronal but not glial cell populations because prominent nSR100 nuclear staining (marked by coincident Hoechst staining) is detected only in the anti-βIII tubulin-positive cells (Figure 2A). Together, these experiments indicate that after neural progenitor cells differentiate, nSR100 primarily functions in the nuclei of neurons.

nSR100 Is Required for Neural Cell Differentiation

We next asked whether nSR100 functions in the differentiation of cultured Neuro2a cells, murine embryonic stem cells (ESCs), and adult neural stem cells. Neuro2a cells produce long extensions known as neurites in the presence of retinoic acid (RA). ESCs can be differentiated to produce neural stem and progenitor cells (Tropepe et al., 2001), and neural stem cells isolated from adult mouse brains can be differentiated into all major cell types of the nervous system in culture (Morshead et al., 1994). These three systems allowed us to investigate the role of nSR100 during different aspects of neural differentiation in vitro.

In Neuro2a cells, nSR100 is expressed prior to induced differentiation and does not significantly increase at 48 hr after induction (data not shown). To test whether nSR100 is required for neurite extension, lentivirus-delivered short hairpin RNAs (shRNAs) were used to generate undifferentiated Neuro2a cells with constitutively reduced (by 70%–75%) levels of nSR100, relative to undifferentiated cells expressing a control shRNA targeted to GFP (Figure 2B). The reduced levels of nSR100 had no significant impact on cell viability (Figure S3 and data not shown), but dramatically impaired neurite extension (Figures 2C and S4). Within 24 hr after induction with RA, >35% of control shRNA-treated cells extended long neurites, whereas only ~5% of the nSR100 shRNA-expressing cells extended processes of

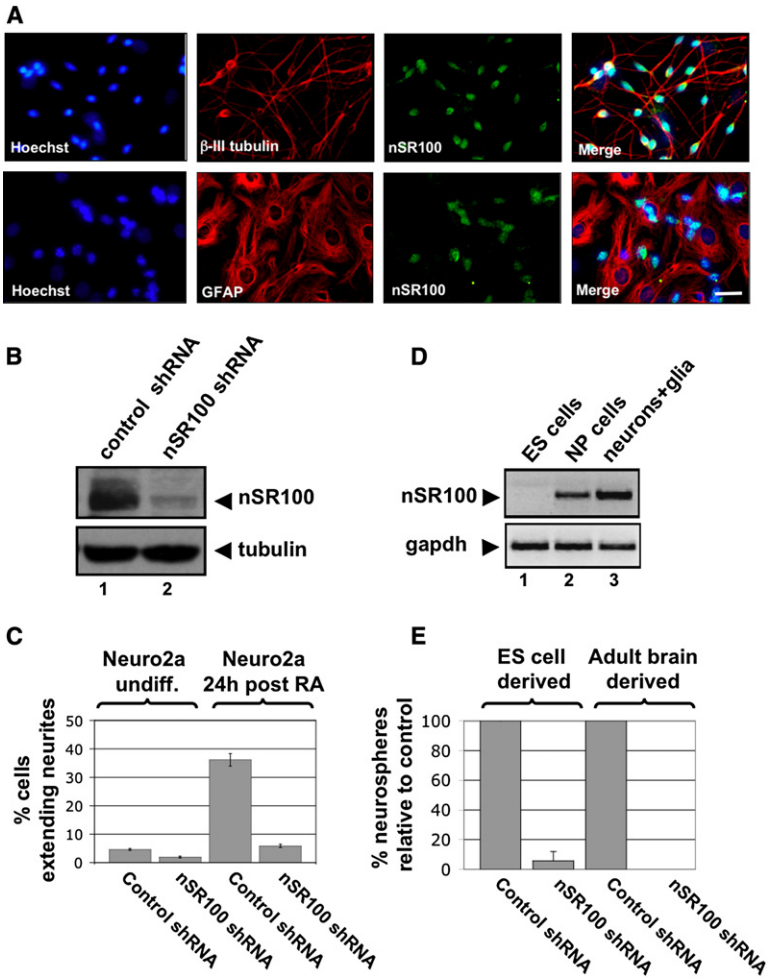

Figure 2. nSR100 Is Required for Neural Cell Differentiation

(A) Confocal microscopy images of differentiated neural progenitor cells coimmunostained with anti-β-III tubulin (red, top panels), anti-glial fibrillary acidic protein (anti-GFAP; red, bottom panels), and anti-nSR100 (green, top and bottom panels) antibodies. Nuclei are stained using Hoechst dye (blue, top and bottom panels). All β-III tubulin-positive neurons show nSR100 staining. Scale bar represents 25 μm.

(B) Western blot probed with anti-nSR100 antibody showing lysates from Neuro2a cells stably expressing control shRNA (lane 1) or nSR100-targeting shRNA (lane 2). α-tubulin levels were used as a loading control.

(C) Quantification of percentage of shRNA-expressing Neuro2a cells extending long neurites (measured as greater than three cell body lengths) under normal culture conditions and differentiation conditions. Values represent averages from three independent experiments ± one standard deviation. Figure S3 shows representative brightfield images of Neuro2a cells from each treatment.

(D) RT-PCR analysis of nSR100 mRNA levels in ES, neural progenitor (NP), and differentiated neurons and glia (lanes 1, 2, and 3, respectively). Gapdh mRNA levels are shown for comparison.

(E) Quantification of relative percentage of primary neurospheres formed by differentiating ESCs expressing control or nSR100-targeting shRNAs or secondary neurospheres from adult neural stem cells expressing control or nSR100-targeting shRNAs. Values represent the averages from four independent experiments ± one standard deviation.

comparable length (Figures 2C and S4). In contrast, knockdown of a widely expressed SR-related splicing factor, SRm160, resulted in reduced viability of undifferentiated Neuro2A cells (Figure S3). These findings suggest that nSR100 is required for specific steps during neural differentiation, rather than for a more general role associated with cell viability.

nSR100 mRNA levels increase when ESCs are induced to differentiate to form neural progenitor cells (Figure 2D). Cultured ESCs were induced to proliferate and aggregate into spherical cell populations known as "neurospheres," which contain neural progenitor cells. When stably expressing control or nSR100-targeting shRNAs prior to induced differentiation, no discernable differences in morphology or proliferation were observed (data not shown). However, when induced, nSR100 knockdown ESCs formed 90% fewer neurospheres than did the control shRNA-treated cells (Figure 2E). Similar results were observed upon knockdown of nSR100 in induced adult-derived neural stem cells (Figure 2E). Two independent shRNAs targeting nSR100 led to similar results, indicating that the effects are specific and not due to off-target effects (data not shown; see also below and Figure 3D). These results therefore indicate that nSR100 plays a critical role in neural stem and progenitor cell formation and/or proliferation, in addition to a role in neurite extension.

nSR100 Regulates a Network of Brain-Specific Alternative Exons

We next investigated whether the effects of nSR100 knockdown on neural cell differentiation are associated with the deregulation of specific AS events. PolyA+ RNA from control and nSR100 shRNA-expressing, undifferentiated Neuro2a cells was profiled using an AS microarray (Figure 3A; refer to the Supplemental Experimental Procedures). AS patterns in adult mouse whole brain and five nonneural tissues were profiled in parallel (Figure 3B). Confidence-ranked percent exon exclusion estimates (%ex; the percentage of transcripts skipping a profiled alternative exon) were determined (Pan et al., 2004). In order to enrich for physiologically relevant events, we focused our analysis on exons displaying both nSR100-dependent regulation in Neuro2a cells and differential splicing between brain and nonneural tissues (Figure 3B and data not shown).

One hundred and fifteen high-confidence AS events met the above criterion and displayed %ex differences of at least 15% upon nSR100 knockdown (Table S2). Seventy percent (81/115) displayed increased exon skipping upon knockdown of nSR100, and RT-PCR experiments validated 81% (21/26) of these events (Figures 3C and S5; data not shown). Only one of seven tested events displaying increased exon inclusion upon nSR100 knockdown was validated, although the change in %ex was relatively modest (data not shown). Moreover, only 6% (3/52) of predicted non-nSR100 targets were found to change upon nSR100 knockdown, indicating a low false-negative detection rate (data not shown). The reduced levels of exon inclusion observed upon

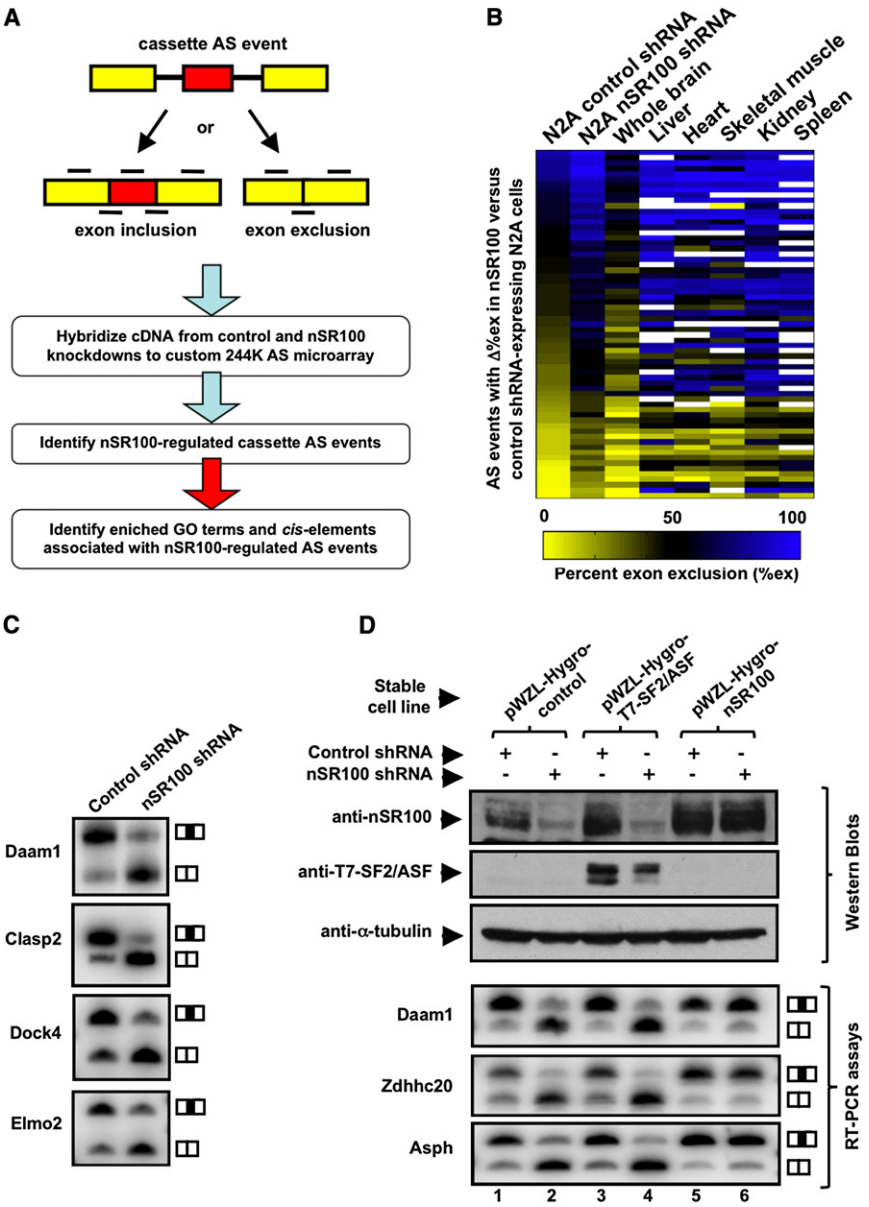

Figure 3. nSR100 Regulates a Network of Neural-Specific Alternative Splicing Events

(A) Strategy used for the global analysis of nSR100-regulated AS. Black lines represent exon body and exon junction probes used to monitor AS levels on a custom microarray.

(B) Heatmap displaying microarray %ex values for a subset of nSR100-regulated alternative exons. Columns show microarray %ex predictions from profiled adult mouse tissues and Neuro2a cells expressing control or nSR100-targeting shRNAs, and rows represent %ex predictions for individual nSR100-regulated exons undergoing increased skipping upon nSR100 knockdown. The AS events are sorted in descending order according to the magnitude of the %ex values in the control shRNA-expressing Neuro2a cells. All AS events displayed have detectable expression in whole brain and at least two other tissues; white indicates expression was below the threshold level used to derive %ex estimates.

(C) RT-PCR assays using primers specific to the constitutive exons flanking nSR100-regulated alternative exons in Daam1, Clasp2, Dock4, and Elmo2 transcripts. Bands corresponding in size to exon-included and exon-skipped isoforms are indicated.

(D) Neuro2a cell lines stably expressing control (lanes 1, 3, and 5) or nSR100 targeting (lanes 2, 4, and 6) shRNAs and pWZL-hygro empty vector (lanes 1 and 2), T7 epitope-tagged SF2/ASF (lanes 3 and 4), or nSR100 cDNA (lanes 5 and 6). Top three panels show western blots monitoring the expression of nSR100 (top panel), T7-tagged SF2/ASF (middle panel), and α-tubulin (bottom panel). Bottom three panels show RT-PCR assays using primers to specifically monitor AS in the Daam1, Zdhhc20, and Asph transcripts.

knockdown of nSR100 persisted following RA-induced differentiation in all of five analyzed cases (Figure S6). These results indicate that nSR100 acts predominantly to promote alternative exon inclusion prior to the formation of neurites in Neuro2a cells.

To address whether the altered exon inclusion levels in the knockdown experiments were specifically caused by the shRNA-reduced expression of nSR100, an RNAi-resistant form of nSR100 mRNA was stably expressed in the nSR100 shRNA knockdown line and splicing levels of several alternative exons were monitored by RT-PCR assays. Expression of nSR100 in the knockdown line, which was confirmed by western blotting (Figure 3D, top panel, lanes 5 and 6), fully restored the inclusion of the tested alternative exons (Figure 3D, lower three panels, compare lanes 5 and 6 with 1–4). In contrast, stable expression of another SR protein, SF2/ASF, did not function in this manner (Figure 3D, all panels, lanes 3 and 4). These results support the conclusion that nSR100 functions specifically to promote exon inclusion. The nSR100-regulated exons were estimated to represent ~11% of AS events identified as being differentially regulated in nervous system tissues by microarray profiling (see the Supplemental Experimental Procedures).

A Gene Ontology annotation enrichment analysis revealed that genes containing nSR100-regulated exons are significantly enriched in functions associated with membrane dynamics and cytoskeleton remodeling (Table S3), processes that are critical for the differentiation of neurons and neurite extension. Also supporting functional significance, nSR100-regulated alternative exons are significantly more often frame preserving (66.7% versus 45.4%; $p < 0.005$, Fisher's exact test) and conserved in human transcripts (62.8% versus 24.5%; $p < 10^{-9}$, Fisher's exact test) than are the other profiled exons (Table S2). These results thus reveal that nSR100 regulates a network of mostly conserved AS events in functionally related genes that play important roles in the formation and function of the nervous system.

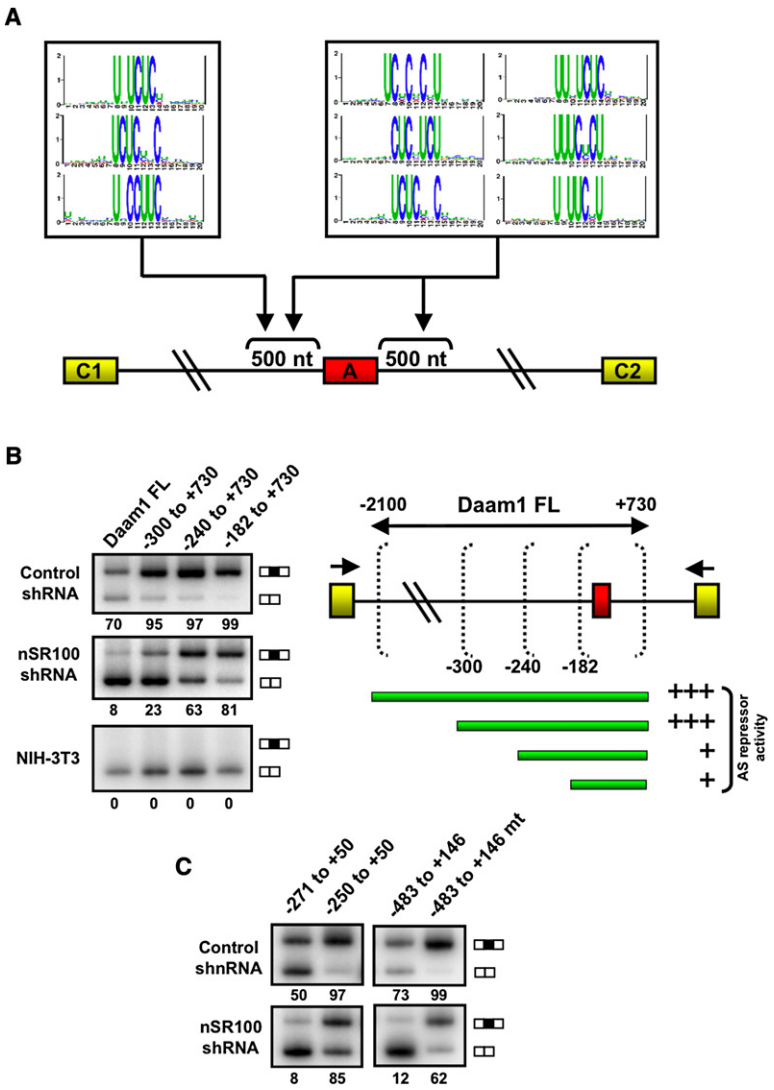

Figure 4. Elements of an nSR100 Regulatory Code

(A) Pyrimidine-rich motifs identified as significantly enriched in the 500 nucleotides of upstream and/or downstream intron sequence flanking nSR100-regulated alternative exons. Motifs with FDR-corrected hypergeometric p value scores <0.01 are shown.

(B) (Left) RT-PCR assays monitoring AS levels of Daam1 exon 16 minigene reporters transfected in NIH 3T3 cells and in Neuro2a cells expressing control or nSR100-targeting shRNAs. The lengths of upstream and downstream intron sequence included in each minigene reporter are indicated above the gel. (Right) The diagram indicates the length of *Daam1* genomic DNA sequence included in each minigene reporter (green bars) and the degree of AS repressor activity associated with these regions (indicated by pluses).

(C) RT-PCR assays monitoring the AS levels of transcripts derived from additional Daam1 minigene reporters in Neuro2a cells expressing control shRNA or nSR100-targeting shRNAs. Gels on the left display AS patterns observed with reporters containing either 271 or 250 nucleotides of upstream intron sequence and 50 nucleotides of downstream intronic sequence. Gels on the right display AS patterns from reporters containing 483 and 146 nucleotides of upstream and downstream sequence, respectively, when region −271 to −250 and additional upstream pyrimidine nucleotides (up to position −280; see Figure S8) are unchanged (−483 to 146) or substituted (−483 to 146 mut) with an unrelated sequence of equal length. Percent exon inclusion levels (%inc) are shown below gel images in (B) and (C).

An nSR100 Regulatory Code

To gain insight into the mechanism by which nSR100 regulates neural-specific AS, we identified motifs of 5–10 nucleotides in length that are significantly enriched in the regulated alternative and adjacent constitutive exons and in the 500 nucleotides of intron sequence that flank these exons (Figure 4A; refer to the Supplemental Experimental Procedures). The most enriched and prevalent motifs are C/U rich and are specifically located within the upstream and/or downstream intronic regions flanking nSR100-regulated exons (Figure 4A, FDR-corrected p value <0.01). Additional high scoring motifs were identified using the same procedure (Figure S7; see the Discussion).

As a parallel approach to defining *cis*-regulatory elements, we generated an AS minigene reporter (Daam1 FL) consisting of a 2.8 kb genomic fragment encompassing nSR100-regulated *Daam1* exon 16 (Figure 4B). *Daam1* is required for neurite formation and outgrowth during development (Matusek et al., 2008), and skipping of exon 16 in nonneuronal cells is predicted to disrupt a formin homology-like domain that likely mediates important interactions with signaling partners and components of the cytoskeleton.

The Daam1 FL minigene reporter recapitulated the AS pattern of endogenous Daam1 transcripts, with the alternative exon displaying more inclusion in Neuro2a cells expressing control shRNAs relative to cells expressing shRNAs targeting nSR100 (Figure 4B). Moreover, the inclusion of Daam1 exon 16 appears to be neural specific because reporter transcripts expressed in NIH 3T3 and myoblast C2C12 cell lines undergo complete exon skipping (Figure 4B and data not shown). These results indicate that *cis* elements required for nSR100-dependent regulation of Daam1 exon 16 are contained within the 2.8 kb Daam1 FL reporter genomic fragment.

Deletion of the Daam1 reporter intron sequences followed by refined mutagenesis revealed a region 250 to 271 nucleotides upstream of the alternative exon that significantly affected nSR100-dependent exon inclusion (Figures 4B and 4C). Deletion of this region resulted in increased exon inclusion. This effect was most pronounced in the nSR100 knockdown cell line (Figure 4C, compare lanes 1 and 2). Similar effects were observed when this region and neighboring nucleotides were substituted with unrelated sequence (Figure 4C, compare lanes 3 and 4). These results indicate that this 21 nucleotide region contains a strong repressor element that results in the skipping of Daam1 exon 16 in the absence of nSR100. nSR100 thus appears to play a critical role in overcoming the repressive effects exerted by this element.

In agreement with our computational analysis, the −271 to −250 AS repressor region and its neighboring nucleotides are

highly enriched in pyrimidine nucleotides (Figure S8) and two of the computationally identified motifs overlap this region. Therefore, both approaches to defining *cis*-regulatory elements strongly implicate pyrimidine-rich motifs in nSR100-dependent splicing regulation.

nSR100 Promotes nPTB Protein Expression

Pyrimidine-rich motifs have previously been implicated in neural-specific regulation of AS involving PTB (also hnRNPI/PTBP1), a widely acting splicing repressor, and its neural-enriched paralog nPTB (also brPTB/PTBP2) (see the Introduction and below). The switch from PTB to nPTB during neuronal differentiation is regulated in part by a neuronal miRNA miR-124 (Makeyev et al., 2007). In nonneuronal cells, expression of PTB results in skipping of exon 10 in nPTB pre-mRNA and this leads to the introduction of a premature termination codon that elicits nonsense-mediated mRNA decay of nPTB transcripts (Boutz et al., 2007; Makeyev et al., 2007; Spellman et al., 2007). In neuronal cells, miR-124 repression of PTB facilitates nPTB exon 10 inclusion and productive nPTB expression.

To address whether PTB and/or nPTB are involved in the regulation of nSR100-dependent AS events, we knocked down these factors individually or together using siRNAs (Figure 5A). As expected, knockdown of PTB led to increased inclusion of exon 10 in nPTB pre-mRNA. RT-PCR assays were then used to monitor the AS levels of Daam1 exon 16 and nine randomly selected, RT-PCR-validated nSR100-regulated exons (Figures 5A and S9).

In contrast to the effect of nSR100 knockdown, Daam1 exon 16 and eight of the nine other exons displayed increased levels of inclusion when PTB levels were reduced and to a lesser extent when nPTB was reduced. Simultaneous depletion of nPTB and PTB resulted in levels of exon inclusion that were at least as high and in some cases higher than the levels observed when PTB was knocked down alone. These findings establish a widespread role for PTB/nPTB in the repression of nSR100-dependent AS events. More specifically, these proteins promote skipping of the same exons that require nSR100 for neural-specific inclusion. Consistent with a previous proposal (Markovtsov et al., 2000), the less repressive activity of nPTB relative to PTB suggests that it might facilitate neural-specific AS by establishing complexes that are more permissive to positive acting factors.

To further explore the functional relationship between nSR100 and PTB/nPTB proteins, we next asked, (1) does nSR100 promote neural-specific AS by regulating the relative levels of nPTB and PTB proteins, (2) do PTB/nPTB bind directly to C/U-rich sequences involved in mediating nSR100-dependent regulation, and (3) does nSR100 act in a dominant-positive manner to counteract the repressive activity of nPTB?

Our microarray profiling experiments (Figure 3) in fact predicted increased skipping of nPTB exon 10 in Neuro2a cells depleted of nSR100 (Table S2). Confirming this prediction, knockdown of nSR100, while not altering PTB mRNA or protein levels, resulted in decreased inclusion of nPTB exon 10 and, consequently, reduced levels of nPTB mRNA and protein (Figure 5B). Consistent with the repressive effects of PTB and nPTB on nSR100-regulated exons, both proteins bind directly and specifically to C/U-rich intron regions upstream of Daam1 exon 16 (Figures S8 and S10). However, essentially no binding to these regions was observed when comparable levels of purified nSR100 (Figure S10A) were added alone or in combination with PTB or nPTB (Figure S11A). At much higher amounts of nSR100, a low level of binding was observed although this appeared to be relatively less specific (Figure S11A).

Further supporting a critical role for nSR100 in promoting neural-specific exon inclusion of PTB/nPTB repressed exons, when nPTB is overexpressed in Neuro2a cells, increased skipping of Daam1 exon 16 is observed (Figure S11B). However, simultaneous overexpression of nSR100 and nPTB effectively alleviates the repressive activity of nPTB and results in ~100% inclusion of Daam1 exon 16 (Figure S11B). This confirms that nSR100 is required to promote the inclusion of neural-specific exons in cells that also express nPTB.

nSR100 Promotes Neural-Specific Exon Inclusion In Vitro

nSR100 appears to act together with nPTB and possibly other factors to promote neural-specific exon inclusion. We next asked whether nSR100 functions in this manner in vitro. Splicing-competent extracts were prepared from neuronal Weri-Rb1 cells and efficiently (>90%) immunodepleted of nSR100 using affinity-purified anti-nSR100 antibody (Figure 1E) or mock-depleted using rabbit anti-mouse antibody (Figure 5C, compare lanes 1 and 2 with lanes 3 and 4). A T7-transcribed, three-exon pre-mRNA consisting of Daam1 exon 16 with 280 nucleotides of upstream and 145 nucleotides of downstream intronic sequence, inserted between strong constitutive exons derived from an adenovirus pre-mRNA substrate (MINX), was assayed for splicing activity in these extracts.

This substrate splices efficiently in the mock-depleted Weri extract, producing exon 16 included and skipped transcripts (Figure 5D, lane 2). When nSR100 is immunodepleted, increased exon 16 skipping is detected (Figure 5D, lane 3), whereas addition of increasing amounts of purified nSR100 protein results in ~100% inclusion of exon 16 (Figure 5D, lanes 4–8). This activity is specific because addition of comparable levels of the SR family protein SF2/ASF (Figure S10A) does not result in a substantial increase in exon 16 inclusion (Figure 5D, compare lanes 4–8 with 9–13). Moreover, addition of purified nSR100 protein to a HeLa splicing extract does not promote the inclusion of Daam1 exon 16 (Figure 5E, compare lanes 2–5 with 6–9). These results demonstrate that nSR100 functions to promote the inclusion of Daam1 exon 16 in a neural cell extract. However, consistent with the results demonstrating that nSR100 functions in part by promoting the expression of nPTB, it is not sufficient to promote a neural-specific splicing pattern in a nonneural extract.

We next performed in vitro and in vivo UV crosslinking followed by immunoprecipitation (CLIP; Supplemental Experimental Procedures) to establish whether, in the context of other cellular factors, nSR100 interacts directly and specifically with its regulated target pre-mRNAs. Anti-nSR100 antibody specifically enriched a radiolabeled protein approximately the size of nSR100 from Weri extract incubated and crosslinked in the presence of a ^{32}P-UTP-labeled Daam1 RNA consisting of the upstream intronic regulatory sequences (Figure 5F, compare lanes 2 and 4).

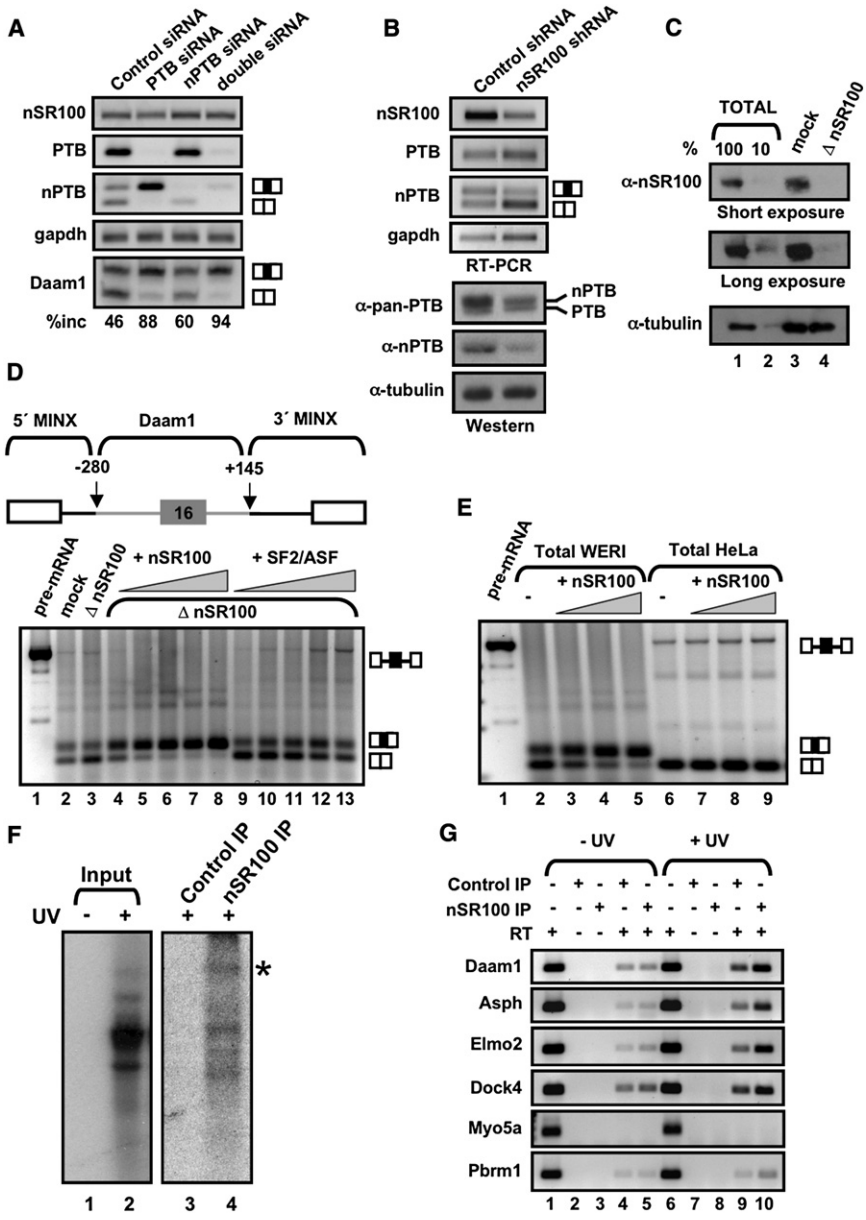

Figure 5. nSR100 Functions by Promoting nPTB Expression and by Binding to its Regulated Target Transcripts

(A) (Left) RT-PCR assays monitoring steady-state mRNA expression levels and AS patterns of nSR100, PTB, nPTB, and Daam1 transcripts in Neuro2a cells transfected with control siRNAs (lane1) or siRNAs targeting PTB, nPTB, or both of these factors. Expression levels of Gapdh transcripts were monitored to control for recovery and loading.

(B) RT-PCR assays monitoring the expression levels and/or AS patterns of nSR100, PTB, nPTB, and Gapdh transcripts in Neuro2a cells expressing control or nSR100-targeting shRNAs (top four panels). Western blotting (bottom three panels) was performed using lysates from the cells assayed in (A) and antibodies capable of detecting PTB paralogs (α-pan-PTB) and nPTB specifically (α-nPTB) (refer to Supplementary Data for additional details). Tubulin levels were monitored to control for sample recovery and loading.

(C) Immunodepletion of nSR100 from splicing competent Weri whole cell extracts. Western blotting on extracts immunodepleted of nSR100 (ΔnSR100) using anti-nSR100 antiserum (lane 4) and mock-immunodepleted (mock) using rabbit anti-mouse antibody (lane 3). Two different amounts of total extract, corresponding to 100% and 10% of the amounts of extract loaded in lanes 3 and 4, are shown in lanes 1 and 2, respectively.

(D) Purified recombinant nSR100 protein specifically promotes the inclusion of Daam1 exon 16 in vitro. A T7 pre-mRNA transcript (see diagram) consisting of strong constitutively spliced 5′ and 3′ exons (MINX) and Daam1 alternative exon 16, flanked by its native upstream and downstream intron sequence, was incubated in the Weri extracts (C) supplemented with and without recombinant proteins (Figure S10A) and splicing activity was monitored by RT-PCR assays and primers specific for the MINX exons. The ΔnSR100 extract was supplemented with 10, 25, 50, 100, and 200 ng of purified nSR100 protein (lanes 4–8, respectively) or with 5, 12.5, 25, 50, and 100 ng of SF2/ASF protein (lanes 9–13). Splicing of the Daam1 pre-mRNA in the mock and ΔnSR100 Weri extracts without added proteins is shown in lanes 2 and 3, respectively. Lane 1 shows input pre-mRNA.

(E) Recombinant nSR100 protein is not sufficient to promote Daam1 exon 16 inclusion in a nonneural origin (HeLa) cell extract. Weri and HeLa cell extracts were incubated without (lanes 2 and 6) or with 10, 25, and 50 ng nSR100 protein, and splicing activity was monitored as described in (D). Input pre-mRNA is shown in lane 1.

(F) Anti-nSR100 antiserum enriches a protein of the approximate size of nSR100 that is UV crosslinked to Daam1 intronic regulatory sequences. A radiolabeled T7 transcript consisting of the upstream intronic regulatory region (nucleotides −280 to −1) of Daam1 exon 16 was incubated under splicing conditions in Weri cell extracts, without (lane 1) or with (lane 2) UV exposure, prior to extensive treatment of the extracts with RNase. Proteins in these extracts were immunoprecipitated with anti-nSR100 (lane 4) or control (lane 3; rabbit anti-mouse antibodies). Total extract and immunoprecipitated proteins were separated on an SDS-PAGE gel, which was dried and exposed to film. The asterisk denotes the crosslinked protein species migrating at approximately the same location as nSR100.

(G) CLIP reveals that nSR100 interacts directly with endogenous pre-mRNA transcript regions overlapping nSR100 regulated exons. Neuro2a cells were exposed (lanes 1–5) or not exposed (lanes 6–10) to UV light. Immunoprecipitation was performed from lysates prepared from the cells using anti-nSR100 antibody (lanes 3, 5, 8, and 10) or a control (rabbit anti-mouse) antibody (lanes 2, 4, 7, and 9). Detection of immunoprecipitated pre-mRNA regions was performed using primer pairs designed to amplify exon-intron regions within the nSR100 target genes *Daam1, Asph, Elmo2,* and *Dock* 4 and as controls to the nontarget genes *Myo5a* (false positive from microarray predictions) and *Pbrm1*. RT was omitted from the PCR reactions in lanes 2, 3, 7, and 8 to control for possible genomic DNA contamination.

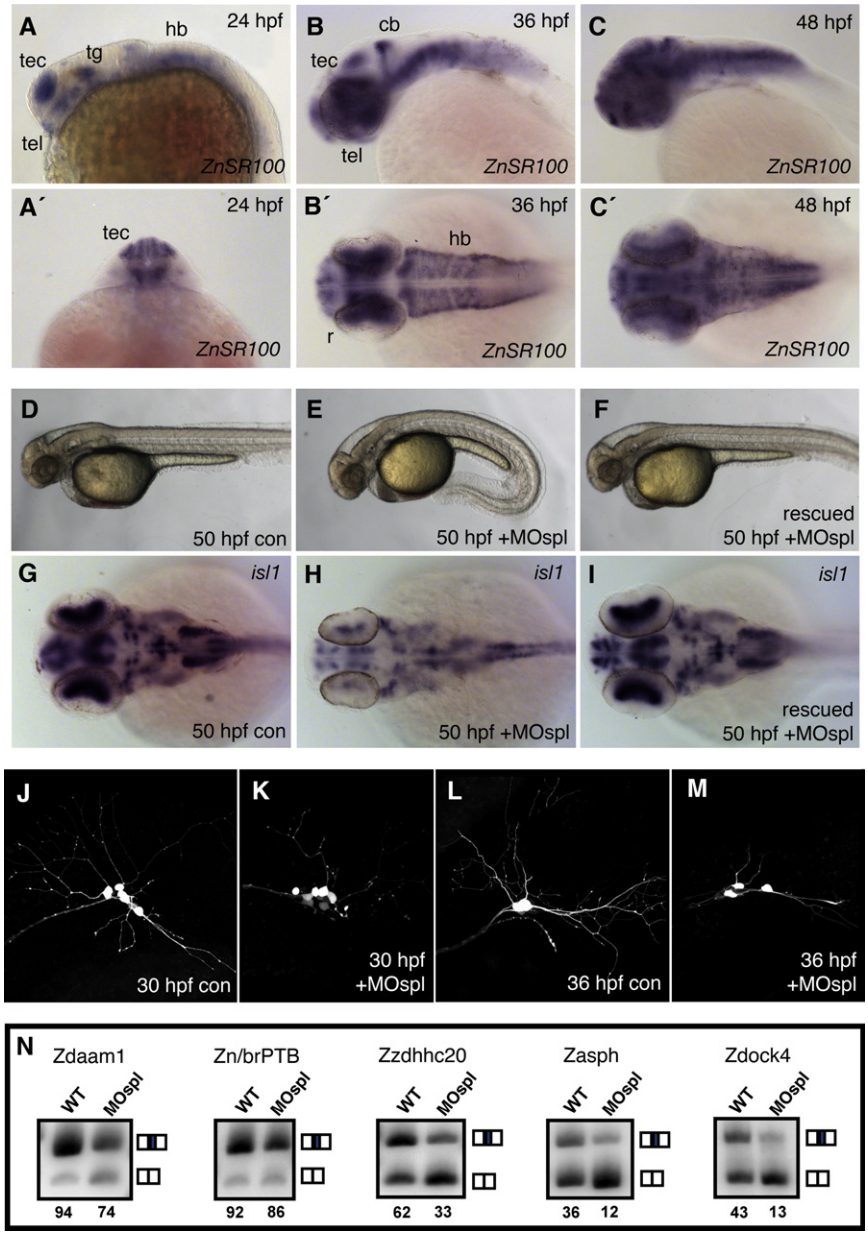

Figure 6. nSR100 Regulates Vertebrate Nervous System and Sensory Organ Development

(A–C) RNA in situ hybridization assays monitoring ZnSR100 expression in the developing zebrafish embryo.

(A and A′) expression at 24 hpf, lateral and frontal views, respectively.

(B and B′) nSR100 expression at 36 hpf, lateral and dorsal views, respectively.

(C and C′) nSR100 expression at 48 hpf, lateral and dorsal views, respectively.

(D) p53 morpholino antisense oligonucleotide (MO) control-injected embryo at 50 hpf.

(E) p53 + ZnSR100 MOspl-injected embryo at 50 hpf.

(F) p53 + ZnSR100 MOspl-injected embryo at 50 hpf, rescued through coinjection of ZnSR100 mRNA.

(G–I) RNA in situ hybridization assays monitoring *islet-1* expression in 50 hpf embryos. p53-MO-injected control (G), nSR100spl morphant embryo (H), and nSR100spl morphant embryo rescued through coinjection of 20 pg ZnSR100 mRNA (I) are shown.

(J–M) Confocal projections of trigeminal ganglion in Tg(sensory:GFP) transgenic embryos. Control embryo at 30 hpf (J), representative nSR100spl morphant embryo at 30 hpf (K), control embryo at 36 hpf (L), and representative nSR100spl morphant embryo at 36 hpf (M) are shown.

(N) nSR100-regulated alternative exons conserved between zebrafish and mouse display altered splicing patterns in nSR100spl morphant embryos, relative to control embryos. Total RNA was isolated from the heads of wild-type and nSR100spl morphant embryos at 50 hpf, and semiquantitative RT-PCR was performed to analyze AS patterns. Percent exon inclusion values are shown below each lane.

Using in vivo CLIP, anti-nSR100 immunoprecipitates were analyzed by RT-PCR assays to detect intron-exon regions overlapping five validated, nSR100-regulated AS events. In all cases, immunoprecipitation of these regions was observed (Figure 5G; representative examples are shown) and was UV and anti-nSR100 antibody dependent (Figure 5G, compare lanes 4 and 5 with 9 and 10). Moreover, little to no anti-nSR100 immunoprecipitation was detected for three regions overlapping profiled AS events that are not regulated by nSR100 (Figure 5G, lower two panels, and data not shown).

The results described above provide evidence that nSR100 establishes neural-specific AS patterns by forming direct interactions with its regulated target transcripts, as well as by promoting increased expression of nPTB.

A Role for nSR100 in Nervous System Development

The high degree of homology (Figure S2) between mammalian and zebrafish nSR100 (ZnSR100) indicates that its function is likely conserved throughout the vertebrate lineage. Accordingly, we next examined the distribution and function of ZnSR100 in developing zebrafish embryos.

ZnSR100 expression was examined by whole-mount RNA in situ hybridization and no expression was detected prior to gastrulation stages (data not shown). At 24 hr postfertilization (hpf), significant expression was observed in the developing brain, including the tectum (tec) and telencephalon (tel) (Figures 6A and 6A′). Expression was also observed around the trigeminal ganglion (tg), at the mid-hindbrain boundary, and throughout the hindbrain (hb). At 36 hpf, additional ZnSR100 expression was observed in the cerebellum (cb) and within the retina (r) (Figures 6B and 6B′). At 48 hpf, stronger and more widespread ZnSR100 expression was detected throughout the developing eyes and

brain (Figures 6C and 6C′). These results are highly consistent with the expression and immunostaining data for mammalian nSR100 (Figures 1 and 2).

To knock down ZnSR100 function we injected single cell-staged embryos with an antisense morpholino oligonucleotide (MOspl) targeted against the 5′ splice site of exon 5 of ZnSR100 pre-mRNA. Severe neural degeneration was observed throughout the brain and spinal cord of 24 hpf embryos (data not shown). This phenotype resembles a common off-target effect of MO injection caused by induction of the p53-dependent cell death pathway and can be circumvented by knockdown of p53 activity (Robu et al., 2007). We therefore coinjected MOspl together with p53-MO. RT-PCR assays confirmed that the MOspl oligonucleotide caused nearly complete disruption of splicing of ZnSR100 exon 5 to exon 6 (Figure S12). We therefore expected efficient knockdown of ZnSR100 function.

At 50 hpf, control embryos injected with relatively high levels of p53-MO alone appeared phenotypically normal (Figure 6D and data not shown). In contrast, over 90% of MOspl-injected "morphant" embryos exhibited consistent developmental abnormalities that included a curved body axis and expanded brain ventricles (n = 200; Figures 6E and S13). To examine neuronal differentiation in nSR100 morphant embryos, we performed RNA in situ hybridization for *islet-1*, a LIM homeodomain-containing transcription factor that is an early marker for the differentiation of diverse neuronal populations. At 24 hpf, *islet-1* expression in ZnSR100 morphants appeared identical to p53-MO-injected controls (Figure S14). Strikingly, *islet-1* expression in 50 hpf nSR100 morphant embryos was markedly reduced, consistent with a severe disruption to neuronal differentiation (Figures 6G and 6H; compare to Figure S14). These effects were not due to significant developmental delay, as general embryonic morphogenesis and patterning appeared normal in nSR100 morphant embryos (Figure S13).

Similar phenotypes as observed in MOspl morphants were observed after injection of a translation-blocking morpholino targeted to the start codon of ZnSR100 (MOatg; data not shown). Moreover, the morphological and neuronal differentiation defects observed in ZnSR100 MOspl-injected embryos could be rescued by coinjecting in vitro transcribed, capped ZnSR100 mRNA (n = 42/52; Figures 6F and 6I). These results further indicate that the observed phenotypes are not due to off-target effects of MO injection, but rather are the specific result of reduced ZnSR100 expression.

We next examined the consequence of knocking down ZnSR100 function on the axonal extension and branching (arborization) of trigeminal sensory neurons. Trigeminal neurons are among the first neurons to develop in vertebrates and begin to display marked arborization at ~16 hpf in zebrafish embryos. To visualize axon arbors in vivo, we utilized Tg(sensory:GFP) transgenic animals that drive GFP expression in Rohon-Beard and trigeminal sensory neurons (Sagasti et al., 2005). Confocal projections of trigeminal ganglia in control embryos at 30 hpf (n = 7) and 36 hpf (n = 6) revealed multiple axonal projections and an elaborate array of peripheral sensory arbors (Figures 6J and 6L). In contrast, visualization of trigeminal sensory neurons in ZnSR100 morphant embryos at 30 hpf (n = 7) and 36 hpf (n = 6) revealed obvious defects in the formation of peripheral sensory arbors (Figures 6K and 6M). As before, these defects could be rescued by coinjection of ZnSR100 mRNA (Figure S15). Together, the results described above indicate a critical role for nSR100 in neuronal differentiation in a whole animal context.

Finally, we analyzed the effects of MOspl disruption of ZnSR100 on the AS levels of exons that are conserved between zebrafish and mouse. Reduced inclusion levels were observed for 6/7 exons that require nSR100 for inclusion in Neuro2A cells, whereas two conserved alternative exons that are not regulated by nSR100 in Neuro2a cells were not affected (Figure 6N and data not shown). These results, which additionally support the specificity of the effects of MOspl-targeting of ZnSR100 function, lead us to conclude that nSR100 regulates a program of AS events that is highly conserved between zebrafish and mammals.

DISCUSSION

A Neural- and Vertebrate-Specific Activator of Alternative Splicing

The discovery and characterization of nSR100 reveals how a large set of brain-specific exons are positively regulated in genes that play numerous critical roles in vertebrate nervous system development. While the evolutionary origin of nSR100 is unclear, its short region of perfect identity with an SRm300 splicing factor-like protein and extensive SR/RS repeat regions (Figure 1) suggests that a duplication event involving an ancestral SRm300-related gene may have led to the emergence of nSR100. Subsequently, nSR100 may have been coadopted with nPTB and other factors to afford the evolution of increased neural AS complexity. Consistent with the evolution of extensive codependent functions, nPTB also appears to have evolved around the time of emergence of the vertebrate lineage (Barbosa-Morais et al., 2006), and both proteins are highly enriched in postmitotic neurons relative to glial cells (Figure 2) (Boutz et al., 2007). These observations support the conclusion that the emergence of nSR100 played a critical role in the evolution of the expanded proteomic and functional complexity of the vertebrate nervous system.

Global and Local Roles for nSR100 in Neural-Specific Alternative Splicing

The global regulatory properties of nSR100 and its remarkably tight neural-restricted expression pattern indicate that it serves as the specificity factor for ~11% of mammalian nervous system-specific AS events (refer to the Supplemental Experimental Procedures). While functioning in conjunction with nPTB, it is possible that nSR100 also functions with other neural-enriched AS regulators such as members of the Fox, CUGBP/CELF, and MBNL families of proteins. In fact, our motif analyses in the present study reveal putative binding sites for several of these factors in the intronic sequences flanking nSR100-regulated exons (Figure S7). Moreover, coimmunoprecipitation experiments reveal that nSR100 associates with specific SR proteins recognized by the pan-SR-specific monoclonal antibody mAb104 (J.A.C, D.O, B.R., and B.J.B, unpublished data).

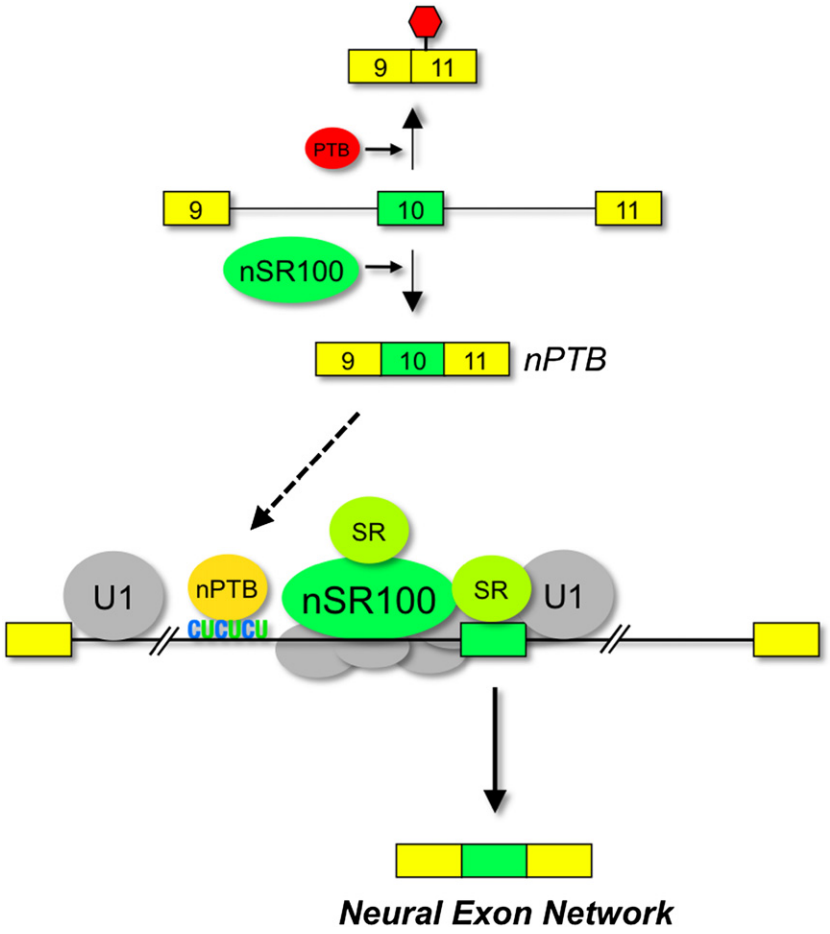

Figure 7. Model for nSR100-Dependent Regulation of Neural-Specific Alternative Splicing

nSR100 activates the inclusion of neural-specific alternative exons in a regulatory circuit that involves the switch between PTB and nPTB proteins. In one part of this circuit, nSR100 promotes the inclusion of exon 10 in nPTB pre-mRNA (green solid arrows), leading to the increased expression of nPTB relative to PTB, which facilitates but is not sufficient for neuronal-specific alternative exon inclusion. In the presence of nPTB and other factors, such as SR family and/or SR-related proteins, nSR100 forges positive-acting interactions by binding to its regulated target transcripts.

Together, these findings support a model (Figure 7) in which nSR100 binds to target transcripts and functions with nPTB and possibly other factors to overcome the repressive forces of PTB during neural differentiation. This model is consistent with emerging evidence for complex regulatory codes involving combinations of different *cis*-regulatory elements bound by corresponding *trans*-acting factors in the regulation of neural-specific AS events (Li et al., 2007). It is also consistent with the established properties of SR family and SR-related proteins, which interact with one another in different contexts to form positive-acting regulatory complexes on pre-mRNA (Lin and Fu, 2007). Indeed, the relatively large size of nSR100 and its extensive RS domains suggests that it could form important interactions with many splicing factors to promote exon inclusion in neural cells.

Functions of an nSR100-Regulated Neural Exon Network

Many nSR100-regulated exons are found in genes required for remodeling of the cytoskeleton, including several with neuronal GTPase activity. Rho family small GTPases are key regulators of the actin cytoskeleton during neuronal morphogenesis and require guanine nucleotide exchange factors for activation (Govek et al., 2005). Besides Daam1, which is required for the activation of the GTPase RhoA (Habas et al., 2001), other nSR100-regulated exons are located in *Dock4* (a guanine nucleotide exchange factor) and its binding partner *Elmo2* (see Figure 3). A complex of Dock4, Elmo2, and adaptor protein CrkII promotes dendritic growth and branching in hippocampal neurons through the activation of another small GTPase, Rac. These observations are consistent with our finding that GTP-based signaling represents one of the most highly enriched functions associated with genes that display nervous system-specific AS (Fagnani et al., 2007). Detailed annotation of the genes with nSR100-regulated exons that have the potential to alter coding sequences reveals that approximately half of the corresponding proteins can be assembled into a network, based on prior published evidence for protein-protein interactions (J. Ellis, J.A.C, and B.J.B, unpublished data). More than half of the regulated exons in this model for an nSR100-regulated network are conserved between human and mouse. It is therefore tempting to speculate that nSR100 target exons function in an elaborate protein-protein interaction network that is critical for remodeling of the cytoskeleton during neuronal differentiation. Future studies will be directed at elucidating the functions of nSR100-regulated AS events.

EXPERIMENTAL PROCEDURES

Identification of RS Domain Protein Genes

Mammalian RS domain genes with tissue-restricted expression patterns were identified using a two-step computational procedure (Figure 1A) coupled to an analysis of mouse mRNA expression profiling data from 50 different cell and tissue types. Refer to Table S1 for a complete annotated list of identified RS domain genes.

Microarray Hybridization, Data Extraction, and Analysis

AS microarray profiling was performed using a new 244 K feature custom oligonucleotide microarray (Agilent Technologies Inc.) representing ~6700 cassette AS events from ~5500 mouse genes. Mining of the AS events and design of the microarray probe sets was performed essentially as described in Pan et al. (2004).

RT-PCR Assays

Nonradioactive RT-PCR assays were performed using the OneStep kit (QIAGEN), and radioactive RT-PCR assays were performed essentially as

described previously (Calarco et al., 2007). Primer sequences are available upon request.

siRNA and Minigene Reporter Transfections

Neuro2a cells were transfected with SMART-pool siRNAs (Dharmacon) using Dharmafect (Dharmacon), as recommended by the manufacturer. Daam1 minigene reporters and expression plasmids were transfected using Lipofectamine 2000 (Invitrogen), as recommended by the manufacturer. Total RNA was collected 48 hr after transfection and isolated using RNeasy kits (QIAGEN).

Recombinant Proteins and RNA Gel Mobility Shift Assays

Purified recombinant proteins were incubated with in vitro-transcribed, radiolabeled transcripts and separated by nondenaturing PAGE. Gels were dried and exposed to X-ray film (Kodak).

In Vitro Splicing Assays

In vitro splicing assays performed in 20 μl contained 1.5 mM ATP, 5 mM creatine phosphate, 5 mM DTT, 3 mM $MgCl_2$, 2.6% PVA, RiboLock RNase inhibitor (Fermentas), 10 ng of splicing substrate, 40–60 μg of Weri or HeLa splicing extract, and up to 12 μL buffer E. Reactions were incubated at 30°C for 1 hr prior to RNA isolation. Spliced products were amplified by RT-PCR assays using primers specific for MINX exons. RT-PCR products were resolved on a 2% ethidium bromide-stained agarose gel stained and visualized using the Gel Doc imaging system (Bio-Rad).

In Vitro Crosslinking and Immunoprecipitation

Weri cell extract was preincubated under splicing conditions in the presence of 60 ng/μL tRNA for 8 min at 30°C. Radiolabeled RNA substrate was added followed by incubation for 15 min at 30°C. Samples were irradiated with UV light for 10 min on ice in a UV Stratalinker 1800 (Stratagene) at a distance of 1.5 cm from the light source, followed by digestion with 0.1 μg of RNaseA for 15 min at 37°C. Samples were separated by SDS-PAGE and analyzed by autoradiography.

Zebrafish Embryo In Situ Hybridization and Oligonucleotide Injections

RNA in situ hybridizations were performed using nitroblue-tetrazolium chloride and 5-bromo-4-chloro-indolyl-phosphate detection (Roche). Embryo staging and analyses were performed using the TLxAB background. One cell stage embryos were injected with 6 ng of antisense morpholino oligonucleotide and 25 pg of capped ZnSR100 mRNA synthesized using the mMESSAGE system (Ambion) as per the manufacturer's recommendation.

ACCESSION NUMBERS

Preprocessed probe intensity scores for all AS microarray data is available from the GEO database under accession number GSE16187.

SUPPLEMENTAL DATA

Supplemental Data include Supplemental Experimental Procedures, three tables, and 15 figures can be found with this article online at http://www.cell.com/supplemental/S0092-8674(09)00711-9.

ACKNOWLEDGMENTS

We are grateful to Leo Lee, Yoseph Barash, Valentina Slobodeniuc, and Xinyi Tang for assistance. We thank many colleagues for providing reagents (Supplemental Data) and to Donny Licatalosi and Robert Darnell for sharing unpublished information and for critical reading of the manuscript. Jim Ingles, Christos Ouzounis, Duncan Odom, Nuno Barbosa-Morais, Arneet Saltzman, Joanna Ip, Jonathan Ellis, and Cori Hanson are also thanked for helpful comments on the manuscript. This work was supported in part by the Canada Research Chairs Program and a grant from the Terry Fox Foundation (#018165) to B.C. Research funding to B.J.B. was provided by a Canadian Institutes of Health Research operating grant (MOP-14609), the Ontario Research Fund, and a grant from Genome Canada through the Ontario Genomics Institute. M.Z. is the recipient of an EJLB scholarship and J.A.C is the recipient of an Alexander Graham Bell Canada graduate scholarship.

Received: November 18, 2008
Revised: March 11, 2009
Accepted: June 1, 2009
Published: September 3, 2009

REFERENCES

Ashiya, M., and Grabowski, P.J. (1997). A neuron-specific splicing switch mediated by an array of pre-mRNA repressor sites: evidence of a regulatory role for the polypyrimidine tract binding protein and a brain-specific PTB counterpart. RNA *3*, 996–1015.

Barbosa-Morais, N.L., Carmo-Fonseca, M., and Aparicio, S. (2006). Systematic genome-wide annotation of spliceosomal proteins reveals differential gene family expansion. Genome Res. *16*, 66–77.

Behrends, U., Schneider, I., Rossler, S., Frauenknecht, H., Golbeck, A., Lechner, B., Eigenstetter, G., Zobywalski, C., Muller-Weihrich, S., Graubner, U., et al. (2003). Novel tumor antigens identified by autologous antibody screening of childhood medulloblastoma cDNA libraries. Int. J. Cancer *106*, 244–251.

Blencowe, B.J. (2006). Alternative splicing: new insights from global analyses. Cell *126*, 37–47.

Boutz, P.L., Stoilov, P., Li, Q., Lin, C.H., Chawla, G., Ostrow, K., Shiue, L., Ares, M., Jr., and Black, D.L. (2007). A post-transcriptional regulatory switch in polypyrimidine tract-binding proteins reprograms alternative splicing in developing neurons. Genes Dev. *21*, 1636–1652.

Calarco, J.A., Xing, Y., Caceres, M., Calarco, J.P., Xiao, X., Pan, Q., Lee, C., Preuss, T.M., and Blencowe, B.J. (2007). Global analysis of alternative splicing differences between humans and chimpanzees. Genes Dev. *21*, 2963–2975.

Fagnani, M., Barash, Y., Ip, J., Misquitta, C., Pan, Q., Saltzman, A.L., Shai, O., Lee, L., Rozenhek, A., Mohammad, N., et al. (2007). Functional coordination of alternative splicing in the mammalian central nervous system. Genome Biol. *8*, R108.

Govek, E.E., Newey, S.E., and Van Aelst, L. (2005). The role of the Rho GTPases in neuronal development. Genes Dev. *19*, 1–49.

Habas, R., Kato, Y., and He, X. (2001). Wnt/Frizzled activation of Rho regulates vertebrate gastrulation and requires a novel Formin homology protein Daam1. Cell *107*, 843–854.

Hanamura, A., Caceres, J.F., Mayeda, A., Franza, B.R., Jr., and Krainer, A.R. (1998). Regulated tissue-specific expression of antagonistic pre-mRNA splicing factors. RNA *4*, 430–444.

Kalsotra, A., Xiao, X., Ward, A.J., Castle, J.C., Johnson, J.M., Burge, C.B., and Cooper, T.A. (2008). A postnatal switch of CELF and MBNL proteins reprograms alternative splicing in the developing heart. Proc. Natl. Acad. Sci. USA *105*, 20333–20338.

Li, Q., Lee, J.A., and Black, D.L. (2007). Neuronal regulation of alternative pre-mRNA splicing. Nat. Rev. Neurosci. *8*, 819–831.

Licatalosi, D.D., Mele, A., Fak, J.J., Ule, J., Kayikci, M., Chi, S.W., Clark, T.A., Schweitzer, A.C., Blume, J.E., Wang, X., et al. (2008). HITS-CLIP yields genome-wide insights into brain alternative RNA processing. Nature *456*, 464–469.

Lin, S., and Fu, X.D. (2007). SR proteins and related factors in alternative splicing. Adv. Exp. Med. Biol. *623*, 107–122.

Makeyev, E.V., Zhang, J., Carrasco, M.A., and Maniatis, T. (2007). The MicroRNA miR-124 promotes neuronal differentiation by triggering brain-specific alternative pre-mRNA splicing. Mol. Cell *27*, 435–448.

Markovtsov, V., Nikolic, J.M., Goldman, J.A., Turck, C.W., Chou, M.Y., and Black, D.L. (2000). Cooperative assembly of an hnRNP complex induced by a tissue-specific homolog of polypyrimidine tract binding protein. Mol. Cell. Biol. *20*, 7463–7479.

Martinez-Contreras, R., Cloutier, P., Shkreta, L., Fisette, J.F., Revil, T., and Chabot, B. (2007). hnRNP proteins and splicing control. Adv. Exp. Med. Biol. *623*, 123–147.

Matusek, T., Gombos, R., Szecsenyi, A., Sanchez-Soriano, N., Czibula, A., Pataki, C., Gedai, A., Prokop, A., Rasko, I., and Mihaly, J. (2008). Formin proteins of the DAAM subfamily play a role during axon growth. J. Neurosci. *28*, 13310–13319.

Morshead, C.M., Reynolds, B.A., Craig, C.G., McBurney, M.W., Staines, W.A., Morassutti, D., Weiss, S., and van der Kooy, D. (1994). Neural stem cells in the adult mammalian forebrain: a relatively quiescent subpopulation of subependymal cells. Neuron *13*, 1071–1082.

Pan, Q., Shai, O., Lee, L.J., Frey, B.J., and Blencowe, B.J. (2008). Deep surveying of alternative splicing complexity in the human transcriptome by high-throughput sequencing. Nat. Genet. *40*, 1413–1415.

Pan, Q., Shai, O., Misquitta, C., Zhang, W., Saltzman, A.L., Mohammad, N., Babak, T., Siu, H., Hughes, T.R., Morris, Q.D., et al. (2004). Revealing global regulatory features of mammalian alternative splicing using a quantitative microarray platform. Mol. Cell *16*, 929–941.

Polydorides, A.D., Okano, H.J., Yang, Y.Y., Stefani, G., and Darnell, R.B. (2000). A brain-enriched polypyrimidine tract-binding protein antagonizes the ability of Nova to regulate neuron-specific alternative splicing. Proc. Natl. Acad. Sci. USA *97*, 6350–6355.

Robu, M.E., Larson, J.D., Nasevicius, A., Beiraghi, S., Brenner, C., Farber, S.A., and Ekker, S.C. (2007). p53 activation by knockdown technologies. PLoS Genet. *3*, e78.

Sagasti, A., Guido, M.R., Raible, D.W., and Schier, A.F. (2005). Repulsive interactions shape the morphologies and functional arrangement of zebrafish peripheral sensory arbors. Curr. Biol. *15*, 804–814.

Shen, H., Kan, J.L., and Green, M.R. (2004). Arginine-serine-rich domains bound at splicing enhancers contact the branchpoint to promote prespliceosome assembly. Mol. Cell *13*, 367–376.

Spellman, R., Llorian, M., and Smith, C.W. (2007). Crossregulation and functional redundancy between the splicing regulator PTB and its paralogs nPTB and ROD1. Mol. Cell *27*, 420–434.

Tropepe, V., Hitoshi, S., Sirard, C., Mak, T.W., Rossant, J., and van der Kooy, D. (2001). Direct neural fate specification from embryonic stem cells: a primitive mammalian neural stem cell stage acquired through a default mechanism. Neuron *30*, 65–78.

Ule, J., and Darnell, R.B. (2006). RNA binding proteins and the regulation of neuronal synaptic plasticity. Curr. Opin. Neurobiol. *16*, 102–110.

Ule, J., Ule, A., Spencer, J., Williams, A., Hu, J.S., Cline, M., Wang, H., Clark, T., Fraser, C., Ruggiu, M., et al. (2005). Nova regulates brain-specific splicing to shape the synapse. Nat. Genet. *37*, 844–852.

Wang, E.T., Sandberg, R., Luo, S., Khrebtukova, I., Zhang, L., Mayr, C., Kingsmore, S.F., Schroth, G.P., and Burge, C.B. (2008). Alternative isoform regulation in human tissue transcriptomes. Nature *456*, 470–476.

Wang, Z., and Burge, C.B. (2008). Splicing regulation: from a parts list of regulatory elements to an integrated splicing code. RNA *14*, 802–813.

Wu, J.Y., and Maniatis, T. (1993). Specific interactions between proteins implicated in splice site selection and regulated alternative splicing. Cell *75*, 1061–1070.

Yeo, G.W., Coufal, N.G., Liang, T.Y., Peng, G.E., Fu, X.D., and Gage, F.H. (2009). An RNA code for the FOX2 splicing regulator revealed by mapping RNA-protein interactions in stem cells. Nat. Struct. Mol. Biol. *16*, 130–137.

Zahler, A.M., Lane, W.S., Stolk, J.A., and Roth, M.B. (1992). SR proteins: a conserved family of pre-mRNA splicing factors. Genes Dev. *6*, 837–847.

Zahler, A.M., Neugebauer, K.M., Lane, W.S., and Roth, M.B. (1993). Distinct functions of SR proteins in alternative splicing. Science *260*, 219–222.

Zhang, C., Zhang, Z., Castle, J., Sun, S., Johnson, J., Krainer, A.R., and Zhang, M.Q. (2008). Defining the regulatory network of the tissue-specific splicing factors Fox-1 and Fox-2. Genes Dev. *22*, 2550–2563.